WARSAW UNIVERSITY OF TECHNOLOGY Index 351733
FACULTY OF CIVIL ENGINEERING
COMMITTEE FOR CIVIL AND WATER ENGINEERING
POLISH ACADEMY OF SCIENCES ISSN 1230-2945

DOI: 10.24425/ace.2023.147655

ARCHIVES OF CIVIL ENGINEERING

Vol. LXIX ISSUE 4 2023 pp. 187 –204

Research paper

Permeability of sandy soils estimated from particle size distribution and field measurements

Wioletta Gorczewska-Langner[1], Anna Gumuła-Kawęcka[2], Beata Jaworska-Szulc[3], Rafael Angulo-Jaramillo[4], Adam Szymkiewicz[5]

Abstract: Accurate estimation of soil permeability is crucial in many geotechnical applications. Empirical and theoretical equations based on soil particle size distribution (PSD) offer a fast and cheap way for preliminary estimation of permeability in granular soils, however the results obtained from various formulas available in the literature often show significant discrepancies. While several comparative studies on this topic have been published, no definite conclusions can be drawn on the performance of the predictive equations in comparison with in-situ permeability measurements. Many formulas require porosity or void ratio as input parameter, which is difficult to obtain for granular soil in-situ. In this study we applied 30 predictive equations to estimate permeability of sandy soil in an outwash plain deposit. The equations were divided into 5 groups, based on their structure and the required input parameters. Empirical formulas were used to estimate the expected in-situ porosity range. The obtained permeability values were compared to the results of in-situ permeameter measurements and pumping tests. Significant differences in the results and in their sensitivity to porosity were found between the 5 groups of methods. In general, simple equations which do not include porosity were in better agreement with measurements than the other groups.

Keywords: groundwater flow, particle size distribution, soil permeability

[1]PhD., Eng., Gdańsk University of Technology, Faculty of Civil and Environmental Engineering, ul. Narutowicza 11, 80-233 Gdańsk, Poland, e-mail: wiogorcz@pg.edu.pl, ORCID: 0000-0001-9907-5528
[2]MSc, Eng., Gdańsk University of Technology, Faculty of Civil and Environmental Engineering, ul. Narutowicza 11, 80-233 Gdańsk, Poland, e-mail: annkawec@pg.edu.pl, ORCID: 0000-0001-6316-7439
[3]DSc., PhD., Eng., Gdańsk University of Technology, Faculty of Civil and Environmental Engineering, ul. Narutowicza 11, 80-233 Gdańsk, Poland, e-mail: bejaw@pg.edu.pl, ORCID: 0000-0003-0082-6120
[4]DR CNRS, DSc., PhD., Laboratoire LEHNA, 3, rue Maurice Audin, 69518 Vaulx-en-Velin, France, e-mail: rafael.angulojaramillo@entpe.fr, ORCID: 0000-0002-9774-1598
[5]Prof., DSc., PhD., Eng., Gdańsk University of Technology, Faculty of Civil and Environmental Engineering, ul. Narutowicza 11, 80-233 Gdańsk, Poland, e-mail: adams@pg.edu.pl, ORCID: 0000-0003-1573-7323

1. Introduction

Permeability of granular (non-cohesive) soils can be estimated from the particle size distribution (PSD) using many formulas developed on empirical or theoretical basis. These equations are useful engineering tools, allowing for prediction of permeability from easily accessible geotechnical data when laboratory or field measurements are not available, e.g. for preliminary evaluation of infiltration capacity of natural and man-made soils and seepage through earth dams and embankments [1, 2]. Reviews of predictive equations can be found in [3–6]. In the last decade new formulas or modifications of the existing ones were proposed by [7–12]. Predictive equations are often developed and validated using laboratory measurements of permeability [6, 10, 13–18], for which accurate information on soil porosity is available. The relationship between porosity and permeability is well recognized [19–21], although the exact form of this dependence is still a subject of research [9, 10]. However, in-situ porosity of granular soils is often difficult to obtain, moreover, in-situ permeability is affected by anisotropy and heterogeneity, which are not represented in the predictive methods. Several authors compared permeability estimates based on PSD to the results of pumping tests [3, 22–25], slug tests [24, 26] and permeameter tests on undisturbed vertical [23, 25, 27] or horizontal [28] cores of sediments. In-situ vertical permeability is generally smaller than the values obtained from PSD [23, 25, 28], but no definite conclusion can be drawn on the relationship between PSD based estimates and in-situ horizontal permeability, which is normally larger than the vertical permeability. Porosity is often estimated using the empirical formula of Vuković and Soro [3, 23, 25, 27, 28], which provides a unique value of porosity depending on the uniformity coefficient obtained from PSD. However, the same soil can have different porosity depending on the compaction state and several empirical formulas are available to estimate the maximum and minimum porosity from PSD, instead of a single value [29, 30].

In this study we applied 30 predictive equations to estimate permeability of sandy soil in an outwash plain deposit. The equations were divided into 5 groups, based on their structure and the required input parameters. Empirical formulas were used to estimate the expected in-situ porosity range. The obtained permeability values were compared to the results of in-situ permeameter measurements and pumping tests. Specific objectives of the work were: (i) to find if there are any systematic differences in the results between the 5 groups of equations, (ii) to evaluate the sensitivity of the equations to porosity as an input parameter and (iii) to find equations which provide the best agreement with the results of field tests in the study area.

2. Materials and methods

2.1. Field measurements

Field measurements were carried out near Cekcyn village in Bory Tucholskie region (northern Poland) as a part of research project focusing on groundwater recharge estimation [31]. In this study we used data from 3 boreholes (P1, P2 and P3), drilled in the

distance of 405 m (P1–P2), 433 m (P1–P3) and 115 m (P2–P3), using machine auger drill. The soil profile, shown in Fig. 1, was similar in each borehole, with a shallow layer of sand (1.5–2 m thick), underlain by a layer of sandy clay (1.5–2 m thick) and a deeper layer of sand, constituting a shallow aquifer with water table at depth of 6–7 m and the aquifer bottom at depth of ca. 15 m. Soil samples for sieve analysis were collected at several depths in the deeper sand layer above and below the water table (P1: 4.0, 6.0, 7.5, 10.0, 12.0, 13.2 m; P2: 4.0, 6.0, 7.5, 9.0, 11.0 m; P3: 3.0, 4.5, 6.0, 8.0, 9.0, 10.5 m). In each borehole an observation well was installed and a pumping test was carried out. Wells were screened in the depth interval 5–11 m and were pumped with a constant rate of about 4.6 m^3/h. The water level was measured in 15-minute intervals until drawdown stabilized. Permeability was calculated based on the Dupuit method with the Forchheimer correction for partial penetration. The radius of drawdown was estimated using the Kusakin empirical formula [32]. Additional measurements were performed with Aardvark permeameter (SoilMoisture Equipment Corp.), in separate boreholes drilled by hand close to each observation well. Measurements were done above the water table in the unsaturated part of the deeper sand layer, at depths 4.5 m in P1 and P2 and 2.8 m in P3. Aardvark is a constant head permeameter, which keeps constant level of water in the borehole (ca. 7.5 cm over

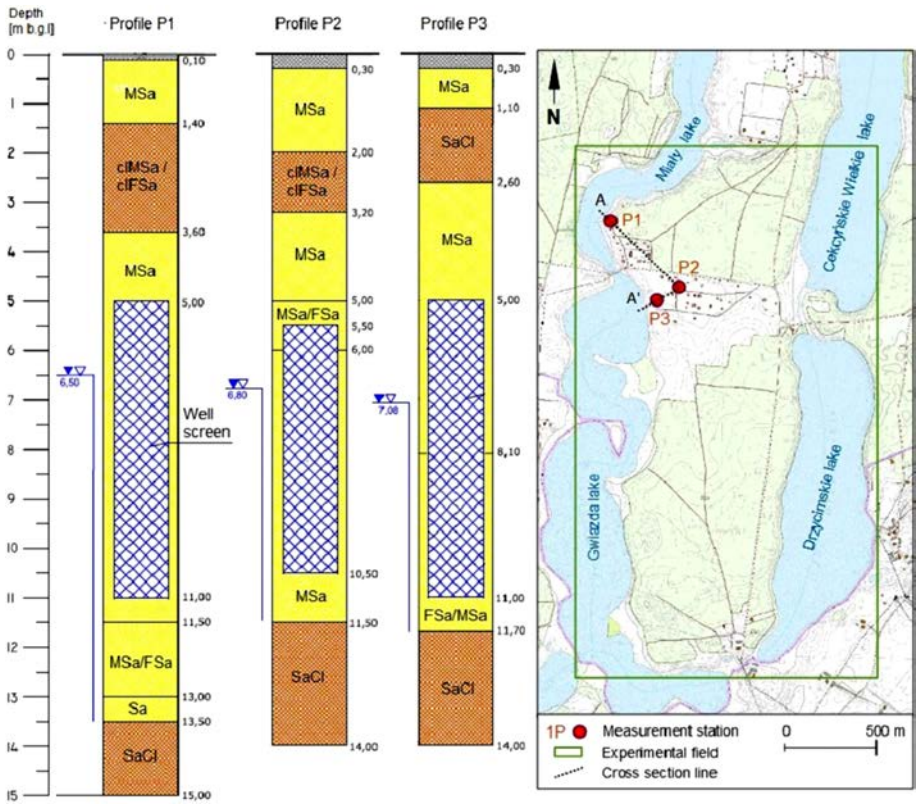

Fig. 1. Lithological profiles of boreholes and map with location of field measurements

the bottom) and imposes radial flow conditions, with fully saturated zone developing near the borehole. Permeability in saturated conditions is obtained from analytical solution of simplified radial flow equation.

2.2. Characterization of soil particles

Particle size distribution for each sample was obtained by sieve analysis, using a standard set of sieves with diameters: 8, 4, 2, 1, 0.5, 0.25, 0.125, 0.063 mm. A toolbox of functions has been developed in Python language to facilitate the calculation of permeability and other soil parameters from the results of sieve analysis. A continuous PSD curve was obtained for each sample using cubic Hermite spline interpolation between the measured points, allowing to compute the diameter d_P corresponding to any given percentage of particles P. The minimum particle diameter (corresponding to zero percentage) was estimated by extrapolating the first segment of the PSD curve. Some formulas require the use of harmonic or geometric average of particle diameters. The harmonic average is defined as:

$$\frac{1}{d_h} = \frac{1}{100\%} \sum_{i=1}^{N} \frac{F^{(i)}}{d_{av}^{(i)}} \qquad \frac{1}{d_{av}^{(i)}} = \frac{1}{3}\left(\frac{1}{d_{\min}^{(i)}} + \frac{2}{d_{\min}^{(i)} + d_{\max}^{(i)}} + \frac{1}{d_{\max}^{(i)}} \right) \tag{2.1}$$

The harmonic average corresponds to the diameter of uniform particles, which have the same specific surface as the considered soil sample [19]. The geometric average is defined as:

$$d_g = \prod_{i=1}^{N} \left(d_{av}^{(i)} \right)^{F^{(i)}/100\%} \qquad d_{av}^{(i)} = \sqrt{d_{\min}^{(i)} \cdot d_{\max}^{(i)}} \tag{2.2}$$

If the distribution of particle diameters resembles log-normal distribution, d_g is close to d_{50}.

Particle shape can be described by sphericity S_F, roundness R_F and shape factor α ($\alpha \geq 6$). Sphericity describes how different is the overall particle shape from a sphere and roundness is a measure of angularity of particle edges. The shape factor α is defined as: $\alpha = A \cdot d/V$, where A – external surface of particle, d – particle diameter (characteristic dimension), V – particle volume. For spherical particles $S_F = 1$, $R_F = 1$ and $\alpha = 6$. For natural sands and gravels $S_F < 1$, $R_F < 1$ and the range of α is reported as 6 to 12 [33]. For an assemblage of particles with the same shape and different sizes the specific surface (per unit volume of particles) can be calculated as $S = A/V = \alpha/d_h$, where d_h is given by Eq. (2.1).

2.3. Estimation of soil porosity

For each soil sample we calculated the minimum ($n_{\min}$) and maximum porosity ($n_{\max}$) as the average of the results of six methods listed in Table 1 (where necessary, void ratio e was converted to porosity n). We assumed that the state of soil in the range of depths from which samples were taken may vary between very dense and medium dense. Thus,

for each soil sample we took $n_{low} = n_{min}$ and $n_{up} = 0.5\,(n_{max} + n_{min})$ as the lower and upper estimate of the expected porosity. These two values were used in the predictive equations for permeability described below.

Table 1. Equations for estimating maximum and minimum porosity or void ratio

Name (acronym) [reference]	Equations
Beyer–Schweiger (BS) [34]	$n_{min} = 0.1537 \cdot (C_U)^{-0.6608} + 0.2305$, $n_{max} = 0.1502 \cdot (C_U)^{-0.6375} + 0.2989$ $C_U = d_{60}/d_{10}$ – uniformity coefficient, analytical equations fitted to the chart from [32] by [3]
Chapuis–Youd (CY) [29, 35]	$\frac{1}{e} = a \ln C_U + b_0 + b_1 R + b_2 R^2 + b_3 R^3$, $a = a_0 + a_1 R + a_2 R^2 + a_3 R^3$ For e_{max}: $a_0 = -0.0931$, $a_1 = 1.9933$, $a_2 = -1.3857$, $a_3 = -0.1457$, $b_0 = -0.1552$, $b_1 = 5.9588$, $b_2 = -8.6685$, $b_3 = 4.3209$, For e_{min}: $a_0 = -0.721$, $a_1 = 8.8518$, $a_2 = -14.623$, $a_3 = 7.9767$, $b_0 = -1.0033$, $b_1 = 17.206$, $b_2 = -32.949$, $b_3 = 21.319$ analytical equations fitted to the chart from [33] by [27]
Kovacs (KOV) [33]	$n = \frac{2}{3} n_1 + \frac{1}{3} n_1 \exp\left(-\frac{C_U - 1}{2}\right)$, $n_1 = n_0 \cdot \left[1 + 10 \cdot n_0^3 \cdot \left(\log_{10} \frac{\alpha}{6}\right)^2\right]$ For n_{min}: $n_0 = 0.38$, for n_{max}: $n_0 = 0.43$
Maroof et al. (MAR) [30]	$e = e_0 \cdot R_F^a \cdot S_F^b \cdot C_U^c$ For e_{min}: $e_0 = 0.5$, $a = -0.3$, $b = -0.26$, $c = -0.2$ For e_{max}: $e_0 = 0.75$, $a = -0.32$, $b = -0.2$, $c = -0.2$
Urish (URI) [36]	$\log_{10}(n) = a + b \log_{10}(d_{50}) + c \log_{10}(d_{90}/d_{10})$ For n_{min}: $a = 1.62563$, $b = -0.08653$, $c = -0.03636$ For n_{max}: $a = 1.53902$, $b = -0.18968$, $c = -0.08201$
Zheng et al. (ZHE) [37]	$e = e_0 \cdot R_F^a \cdot S_F^b \cdot C_U^c$ For e_{min}: $e_0 = 0.5$, $a = -0.15$, $b = -0.25$, $c = -0.15$ For e_{max}: $e_0 = 0.75$, $a = -0.2$, $b = -0.25$, $c = -0.1$

2.4. Predictive equations for permeability

Permeability of granular materials is often expressed by the Kozeny–Carman equation, developed from theoretical principles of laminar flow in porous media [19, 38, 39]:

$$k = \frac{\gamma_w}{\mu_w} \cdot \frac{1}{\xi \cdot \tau \cdot S^2} \cdot \frac{n^3}{(1-n)^2} = \frac{\gamma_w}{\mu_w} \cdot \frac{1}{\xi \cdot \tau \cdot \alpha^2} \cdot \frac{n^3}{(1-n)^2} \cdot d_h^2 = \frac{\gamma_w}{\mu_w} \cdot \frac{1}{\xi \cdot \tau \cdot \alpha^2} \cdot \frac{e^3}{1+e} \cdot d_h^2 \tag{2.3}$$

where: k – permeability (hydraulic conductivity) [m/s], γ_w – specific weight of water [N/m^3], μ_w – dynamic viscosity of water [Pa·s], ξ – coefficient related to pore shape [–], τ – tortuosity [–] (for spherical particles $\xi \cdot \tau = 5$ is commonly assumed [38]).

Eq. (2.3) is dimensionally consistent and states that permeability is proportional to the square of effective particle diameter, defined as harmonic average. Moreover, k depends on fluid properties, pore geometry and porosity n or void ratio e. Eq. (2.3) can be used as a reference for numerous other equations proposed to estimate k from PSD. They can be divided into 5 groups, based on their structure and the required input data (Table 2). Group 1 includes equations which closely resemble Eq. (2.3). They account for the specific surface of particles by using harmonic average of particle diameter, Eq. (2.1), and include porosity or void ratio. Equations in group 2 include the dependence on porosity and square of particle diameter. However, instead of d_h they use diameters corresponding to specific percentages on PSD curve, e.g. d_{10}. Group 3 differs from group 2 by using particle diameters raised to powers different than 2. Thus, equations in group 3 are not consistent dimensionally. Group 4 includes only 2 methods, which do not explicitly account for porosity, but provide different k estimates for loose, medium dense and dense soils. Equations in group 5 do not include porosity. All equations are listed in Table 2 in a unified form, which provides k in [m/s] for d in [mm], γ_w in [N/m^3] and μ_w [Pa·s].

Table 2. Equations for predicting permeability

Name (acronym) [reference]	Equation and comments
Group 1	
Kozeny–Carman (KC) [19, 38, 39]	Eq. (2.3) with $\xi \cdot \tau = 5$ and $\alpha = 9$
Kozeny–Carman-Kimura (KCK) [8]	Eq. (2.3) with $\alpha = 6$, $\xi = 92.9n^{3.04}$, $\tau = n^{1-m}$, m – cementation exponent, $m = 1.505n + 0.984$ $0.132 \text{ mm} \le d_{10} \le 0.509 \text{ mm}$, $0.348 \le n \le 0.444$
Krüger (KRU) [3, 32]	$k = \frac{\gamma_w}{\mu_w} \cdot 4.968 \cdot 10^{-10} \cdot \frac{n}{(1-n)^2} \cdot d_h^2$ $0.32 \le n \le 0.47$, $0.06 \text{ mm} \le d_{10} \le 0.28 \text{ mm}$
Revil–Cathles (RC) [40]	$k = \frac{\gamma_w}{\mu_w} \cdot \frac{1}{24} n^{5.1} \cdot d_h^2$
Revil–Cathles–Kimura (RCK) [8]	$k = \frac{\gamma_w}{\mu_w} \cdot \frac{1}{4\,a\,m^2} \cdot \frac{n^{3m}}{(1-n^m)^2} \cdot d_h^2$ with $a = 17.8n - 2.79$, $m = 1.505n + 0.984$ $0.132 \text{ mm} \le d_{10} \le 0.509 \text{ mm}$, $0.348 \le n \le 0.444$
Slichter (SLI) [3, 20]	$k = \frac{\gamma_w}{\mu_w} \cdot 1.039 \cdot 10^{-8} \cdot n^{3.287} \cdot d_h^2$ The original paper [20] and [41, 42] support the use of d_h instead of d_{10}, as often reported in the literature; n function fitted by [3]
Zamarin (ZAM) [3, 32]	$k = \frac{\gamma_w}{\mu_w} \cdot 6.317 \cdot 10^{-9} \cdot \frac{(1.275 - 1.5 \cdot n)^2 \cdot n^3}{(1-n)^2} \cdot d_h^2$

Continued on next page

Table 2 – *Continued from previous page*

Name (acronym) [reference]	Equation and comments
Zuber (ZUB) [43]	$k = \frac{\gamma_w}{\mu_w} \cdot \frac{3.020 \cdot 10^{-9}}{758.28 \cdot n^3 - 837.69 \cdot n^2 + 261.14 \cdot n - 15.263} \cdot d_h^2$
Zunker (ZUN) [21]	$k = \frac{\gamma_w}{\mu_w} \cdot 1.541 \cdot 10^{-9} \cdot C \cdot \frac{n^2}{(1-n)^2} \cdot d_h^2$ $C = 0.45$ to 1.55, depending on grain shape and uniformity [3, 32], $C = 1.23$ in this study
Group 2	
Diaz–Curiel et al. (DC) [12]	$k = \frac{\gamma_w}{\mu_w} \cdot \frac{4.383 \cdot 10^{-9}}{(d_{75}/d_{25})} \cdot \frac{n^3}{(1-n)^2} \cdot d_{50}^2$
Hazen–Chapuis (HC) [44]	$k = \frac{\gamma_w}{\mu_w} \cdot 1.544 \cdot 10^{-9} \cdot \frac{e^3\left(1+e_{\max}^3\right)}{\left(1+e^3\right)e_{\max}^3} \cdot d_{10}^2$ $C_U \leq 5$, 0.1 mm $\leq$ d10 $\leq$ 3 mm
Mbonimpa et al. (MBO) [45]	$k = \frac{\gamma_w}{\mu_w} \cdot 10^{-8} \cdot \sqrt[3]{C_U} \cdot \frac{e^5}{1+e} \cdot d_{10}^2$
Palagin (PAL) [46]	$k = \frac{\gamma_w}{\mu_w} \cdot \frac{1.757 \cdot 10^{-10}}{0.0243 \cdot C_U^{2.18} + 0.260} \cdot n \cdot d_{10}^2$ if $C_U \leq 3$) $k = \frac{\gamma_w}{\mu_w} \cdot \frac{1.757 \cdot 10^{-10}}{0.109 \cdot C_U^{1.77} + 0.396} \cdot n \cdot d_{10}^2$ if $C_U > 3$) $C_U \leq 19$, 0.16 mm $\leq d50 \leq$ 140 mm
Pavchich (PAV) [47]	$k = \frac{\gamma_w}{\mu_w} \cdot 4.391 \cdot 10^{-9} \cdot \sqrt[3]{C_U} \cdot \frac{n^3}{(1-n)^2} \cdot d_{17}^2$
Ren-Santamarina (RS) [9]	$k = \frac{\gamma_w}{\mu_w} \cdot 1.812 \cdot 10^{-8} \cdot \frac{(\gamma_s/\gamma_w)^2}{(C_U+7)^2} \cdot e^5 \cdot d_{50}^2$ γ_s – specific weight of solid particles, $\gamma_s = 2650$ kg/m^3 in this study
Sauerbrei (SAU) [3, 48]	$k = \frac{\gamma_w}{\mu_w} \cdot 4.746 \cdot 10^{-9} \cdot \frac{n^3}{(1-n)^2} \cdot d_{17}^2$
Terzaghi (TER) [49]	$k = \frac{\gamma_w}{\mu_w} \cdot 10^{-8} \cdot C \cdot \left(\frac{n-0.13}{\sqrt[3]{1-n}}\right)^2 \cdot d_{10}^2$ $C = 1.065$ for rounded grains, $C = 0.612$ for angular grains, $C = 0.839$ in this study
Group 3	
Arshad (ARS) [10]	$k = \frac{\gamma_w}{\mu_w} \cdot 1.019 \cdot 10^{-7} \cdot e^{6.7} \cdot d_C^{3.35}$ $d_C = 0.3d_{10} + 0.2d_{30} + 0.3d_{50} + 0.2d_{60}$ $0.01 < d_{10} < 0.5$, $1.6 < C_U < 12.5$, $0.32 < e < 0.60$

Continued on next page

Table 2 – *Continued from previous page*

Name (acronym) [reference]	Equation and comments
Chapuis (CHA) [44]	$k = \frac{\gamma_w}{\mu_w} \cdot 2.510 \cdot 10^{-9} \cdot \left(\frac{n^3}{(1-n)^2}\right)^{0.7825} \cdot d_{10}^{1.565}$ $0.003 < d_{10} < 3, 0.3 < e < 1$
NAVFAC [44]	$k = \frac{\gamma_w}{\mu_w} \cdot 1.019 \cdot 10^{-9} \cdot 10^{1.291e-0.6435} \cdot (d_{10})^{10^{0.5504-0.2937e}}$ $2 < C_U < 12, d_{10}/d_5 < 1.4, 0.1 < d_{10}$ [mm]$< 2, 0.3 < e < 0.7$
Shahabi (SHA) [50]	$k = \frac{\gamma_w}{\mu_w} \cdot 1.223 \cdot 10^{-9} \cdot C_U^{0.735} \frac{n^3}{(1-n)^2} \cdot d_{10}^{0.89}$ $1.2 < C_U < 8, 0.15 < d_{10}$ [mm] $< 0.59, 0.38 < e < 0.73$
Group 4	
Beyer (BEY) [34, 51]	$k = \frac{\gamma_w}{\mu_w} \cdot 10^{-9} \cdot a \cdot C_U^b \cdot d_{10}^2$ For loose soil $a = 2.288$, $b = -0.1488$, for medium dense soil a =1.835, $b = -0.2006$, for dense soil $a = 1.552$, $b = -0.2312$, (coefficients fitted to the chart in [32] by [3]) $C_U \leq 20$, 0.06 mm $\leq d10 \leq$ 0.6 mm
Prugh (PRU) [52]	k interpolated as a function of d_{50}, C_U and relative density (loose, medium or dense) from digitized plots published in [52] $C_U \leq 10$, 0.05 mm $\leq d_{50} \leq$ 4 mm
Group 5	
Hazen (HAZ) [53]	$k = \frac{\gamma_w}{\mu_w} \cdot 1.544 \cdot 10^{-9} \cdot d_{10}^2$ $C_U \leq 5$, 0.1 mm $\leq d10 \leq$ 3 mm, material in loose state
Krumbein and Monk (KM) [54, 55]	$k = \frac{\gamma_w}{\mu_w} \cdot 7.751 \cdot 10^{-10} \cdot \exp(-1.31 \cdot \sigma) \cdot (d_g)^2$ $\sigma = \frac{\log_2 d_{84} - \log_2 d_{16}}{4} + \frac{\log_2 d_{95} - \log_2 d_5}{6.6}$ $0.04 \leq \sigma \leq 0.80$, 0.273 mm $\leq d_g \leq$ 1.69 mm, $n \approx 0.4$
Seelheim (SEE) [3, 32]	$k = \frac{\gamma_w}{\mu_w} \cdot 4.746 \cdot 10^{-10} \cdot d_{50}^2$ this formula is commonly reported in literature, but not consistent with the original paper [56], see also [22]
Urumović and Urumović (URU) [7]	$k = \frac{\gamma_w}{\mu_w} \cdot 5.555 \cdot 10^{-9} \cdot \frac{n_e^3}{(1-n_e)^2} \cdot d_g^2$ n_e – effective porosity, obtained as a function of d_g and C_U from the chart in [7] (digitized by the authors of this study), 0.0015 mm $\leq d_g \leq$ 6 mm

Continued on next page

Table 2 – *Continued from previous page*

Name (acronym) [reference]	Equation and comments
USBR [11]	$k = \frac{\gamma_w}{\mu_w} \cdot 4.793 \cdot 10^{-10} \cdot d_{20}^{2.3}$, 0.01 mm $\leq d_{20} \leq$ 2 mm
USCRO [11]	$k = \frac{\gamma_w}{\mu_w} \cdot 1.558 \cdot 10^{-9} \cdot d_{20}^{2.32}$, $C_U < 5$
Zieschang (ZIE) [57]	$k = \frac{\gamma_w}{\mu_w} \cdot 1.331 \cdot 10^{-7} \cdot C_1 \cdot (C_2 + C_3) \cdot d_{10}^2$ $C_1 = -0.030073 \ln d_{60} + 0.981765 \quad C_2 = 0.013346 C_U^{-0.130096}$ $C_3 = 0.00024 \sin\left(1.179982\sqrt{C_U} - 0.499419\right)$ $C_U \leq 25$, 0.1 mm $\leq d_{10} \leq$ 0.4 mm, coefficients C_1, C_2, C_3 fitted by [58]

For each sample permeability was evaluated using all equations. For groups 1–3 k was calculated separately for the upper and lower porosity estimate, as described in Section 2.3. In group 4 permeability was calculated assuming medium dense and dense packing. In all formulas in group 1 we used the same value of d_h. As the second step, we calculated average permeability in each profile for each equation, as an arithmetic average for all samples in the profile, evaluated with the considered equation. In groups 1–4 the profile averages were calculated for both upper and lower porosity. The profile averages were compared to the results of field measurements.

3. Results

3.1. Field measurements of permeability

The following values of horizontal permeability [m/s] were obtained from pumping tests: $4.97 \cdot 10^{-4}$ (P1), $5.19 \cdot 10^{-4}$ (P2), $3.55 \cdot 10^{-4}$ (P3). The measurements with Aardvark permeameter provided the following results: $3.68 \cdot 10^{-4}$ (P1), $3.53 \cdot 10^{-4}$ (P2) and $3.73 \cdot 10^{-4}$ (P3). The differences in results are relatively small, which suggests high similarity between all 3 profiles. In P1 and P2 k from permeameter tests was lower than from the pumping tests, probably due to higher degree of anisotropy, which increases k in horizontal direction compared to the average value for radial flow. In P3 both methods yielded essentially the same value of k.

3.2. Particle characteristics and porosity estimates

The three profiles have similar characteristics of grain size distribution, as shown in Table 3 and in Fig. 2. Out of 16 samples, 14 were classified as medium sand (MSa), 4 were on the boundary between fine and medium sand (FSa/MSa) and one was non-uniform sand (Sa). Based on visual inspection of grains and comparison with the widely used Krumbein-Sloss chart [59], S_F was estimated as 0.7 and R_F as 0.5. We assumed $\alpha = 9$,

which is the average of the range reported by [33]. Similar value of α can be obtained from the experiments of [35] on sand having S_F and R_F close to the sand in our study area. Consistently with this choice of α, in the formulas of Zunker and Terzaghi the geometry dependent coefficient was set to the average value between rounded and angular grains.

Table 3. Particle size distribution characteristics (min-max range and average)

Parameter	P1	P2	P3
d_{10} [mm]	0.082–0.161 (0.125)	0.144–0.218 (0.169)	0.116–0.208 (0.159)
d_{50} [mm]	0.202–0.485 (0.285)	0.203–0.387 (0.299)	0.193–0.353 (0.289)
C_U	1.73–5.31 (2.82)	1.49–2.52 (1.96)	1.72–2.42 (1.98)

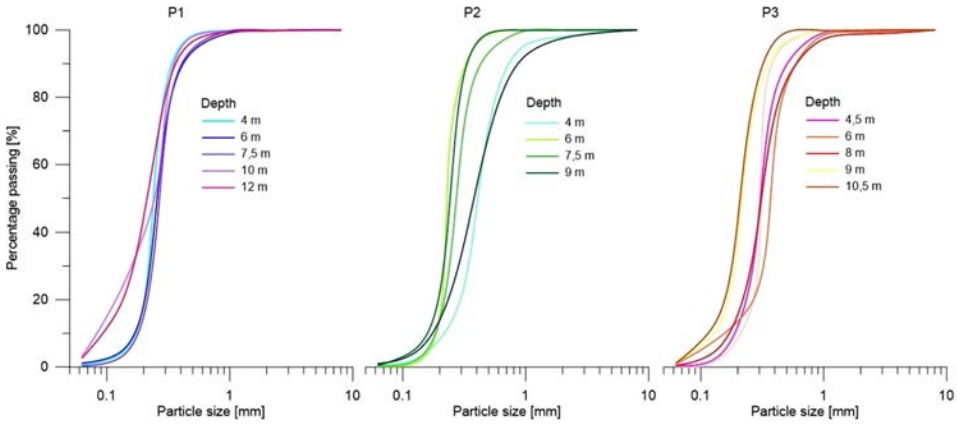

Fig. 2. Particle size distribution curves for the sand samples in profiles

Figure 3 compares the minimum and maximum porosity obtained with 6 empirical formulas (average for each profile). Significant differences exist between methods, with CY, MAR and ZHE providing a much wider range between maximum and minimum values than the other three methods. In all profiles the lowest minimum porosity is obtained with CY and the highest minimum porosity with URI. The maximum porosity according to MAR, URI and ZHE formulas is similar and considerably higher than in the other three formulas. By averaging the 6 formulas for each sample as described above, we obtained lower porosity estimates (n_{low}, very dense state) in soil samples ranging from 0.315 to 0.362 and the upper porosity estimates (n_{high}, medium dense state) ranging from 0.358 to 0.403. This range of values is in good agreement with porosity measured on undisturbed soil samples in the lower part of the shallow sand layer (n = 0.315 to 0.385), characterized by similar grain size distribution as the deeper layer (d_{10} = 0.152 to 0.178 mm, d_{50} = 0.276 to 0.367 mm, C_U = 2.04 to 2.46).

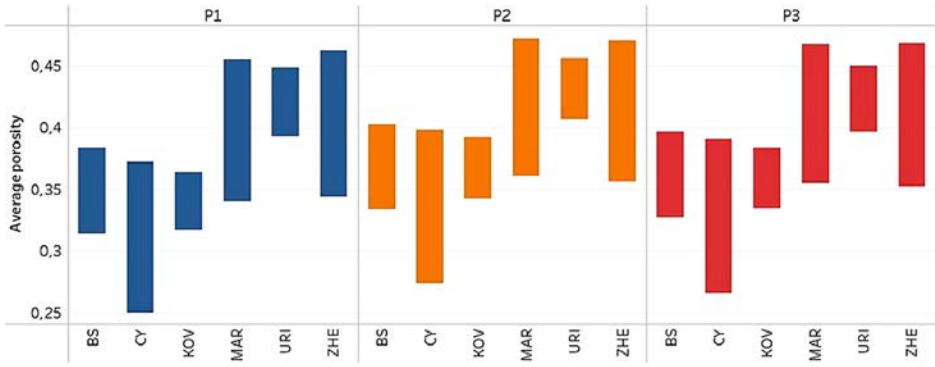

Fig. 3. Average porosity range in each profile estimated from PSD using different methods

3.3. Permeability estimates

Figure 4 shows the average permeability obtained for each profile using different methods in comparison to the values obtained from field measurements. For groups 1–4 the range between results obtained with higher and lower porosity estimates is shown.

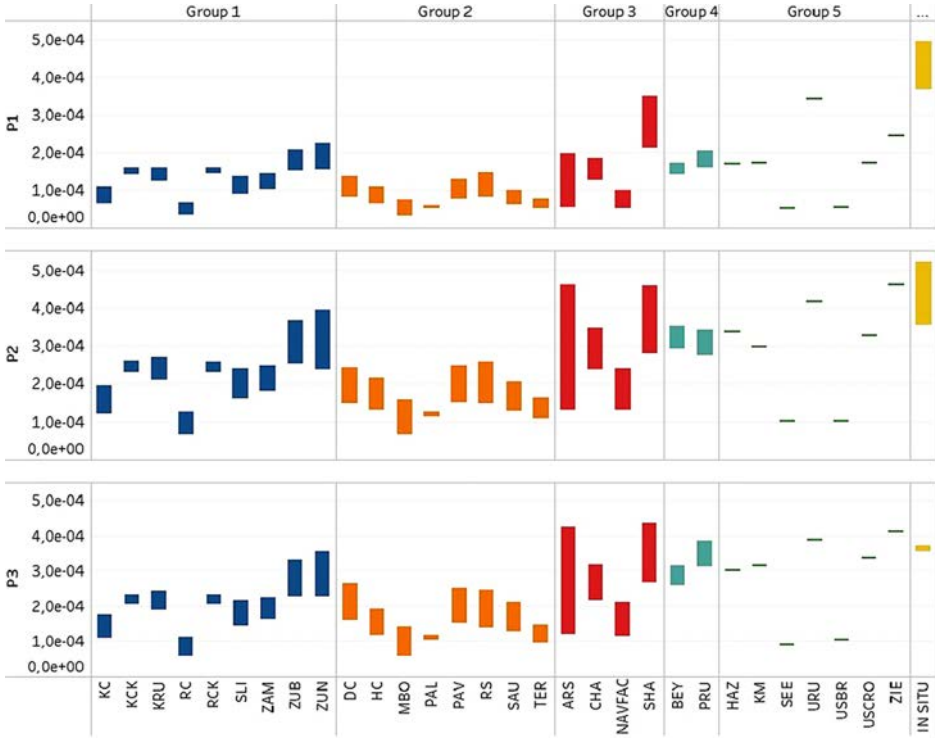

Fig. 4. Average permeability in each profile obtained from PSD and in-situ measurements

Significant differences between groups can be seen and their pattern is very similar for all profiles. The largest scatter of the results occurs in groups 3 and 5 and the smallest in group 4, where BEY and PRU methods show a high degree of consistency. Similarity between various predictive equations can be further explored using hierarchical clustering algorithm [60, 61], which produced the dendrogram shown in Fig. 5. Formulas connected with the shortest lines show the highest similarity. For example, very high similarity occurs between KCK and RCK equations, between DC and PAV equations and between SEE and USBR equations. Two large clusters can be distinguished in Fig. 5, the first one containing equations from KC to RS and the second one – equations from ZUB to PRU. Note however, that in-situ measurements and some methods from groups 3 and 5 fall outside these two clusters. The methods URU and ZIE provide results closest to the measured k values. This is further confirmed by Fig. 6, which shows the average ratio of permeability predicted with each equation to the average permeability obtained from measurements. All equations predict average k lower than the measured values. The best agreement was obtained for URU (0.942), ZIE (0.923) and SHA (0.820). The worst agreement resulted for RC (0.180), SEE (0.206), MBO (0.218) and USBR (0.221). With respect to group averages, the best fit was in group 4 (0.663) followed by group 5 (0.616), while the worst in group 2 (0.320). However, if SEE and USBR are excluded from group 5, the average ratio for this group increases to 0.777, which means that the predictions differ from measurements by less than 25%.

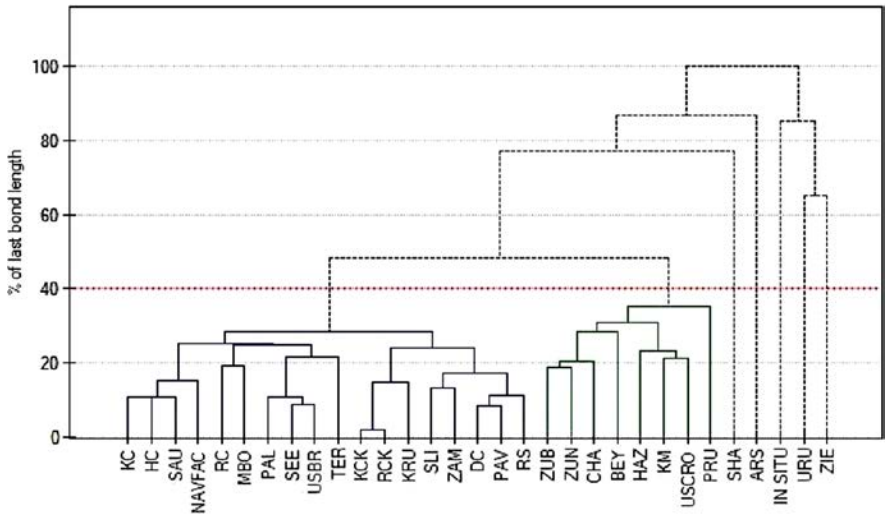

Fig. 5. Dendrogram showing similarities between predictive equations

The formulas significantly differ in their sensitivity to porosity, as shown in Fig. 7. The largest sensitivity is shown by ARS and MBO, for which the higher permeability estimates are on average larger than lower estimates by factors 3.54 and 2.67, respectively. In contrast, RKC, KCK and PAL are the least sensitive, with the upper and lower estimates differing

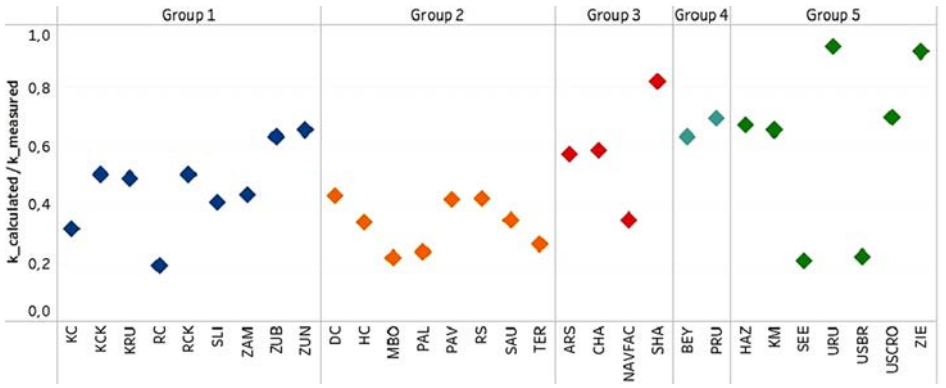

Fig. 6. Ratio of calculated to measured permeability for different predictive equations

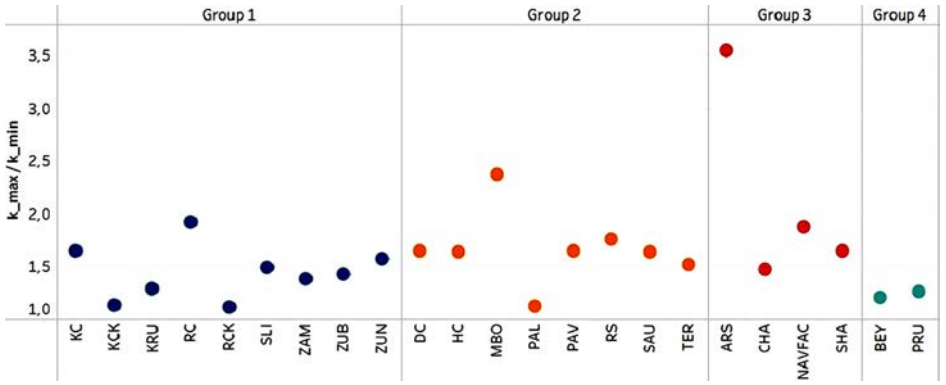

Fig. 7. Sensitivity of predictive equations to porosity

by a factor of less than 1.15. Comparing the average sensitivity in each group, the highest one is in group 3 (2.13) and the lowest one in group 4 (1.23).

4. Conclusions

The best agreement between predictions and in-situ measurements was obtained for those groups of formulas which do not include porosity (Group 5) or account only for the relative density (Group 4). Among 10 equations which showed the best performance, 5 methods from groups 4 and 5 were originally developed using field test results (ZIE, URU, USCRO, PRU, BEY), 2 methods were developed using laboratory results on samples in loose state (HAZ, KM) and only 3 methods explicitly consider porosity (SHA, ZUB, ZUN). Most of the methods based on laboratory measurements predict k lower than in-situ measurements. There are two possible reasons for this. First, the in-situ porosity may be larger than estimated in this work, although, as described in Section 3.2, field

investigations do not seem to support very high porosity values. The second, and seemingly more plausible reason is anisotropy and heterogeneity of soil, which increases in-situ horizontal permeability in many sediments, due to the presence of small-scale horizontal layers or lenses. These features are difficult to capture by formulas based on PSD curves. Accordingly, formulas which were calibrated to the results of field tests generally show better performance than those calibrated to the results of laboratory experiments.

The limitations of the present analysis must be clearly stated. All investigated samples had uniform grain size distribution with $C_U < 6$. The considered predictive equations can be expected to perform quite differently for less uniform PSD [5]. An important source of uncertainty is the lack of reliable data on in-situ sand porosity. This could be provided by in-situ penetration tests (DP or CPT) and laboratory measurements of minimum and maximum void ratio, which unfortunately were not available for this study. Also, we did not perform laboratory test to measure permeability of soil samples at different levels of compaction, which could be compared to the results of field tests. A significant number of laboratory tests performed on sands and other media showed clear dependence of permeability on porosity, e.g. [6, 17]. Thus, we expect that such a dependence would also occur for sandy soils considered in our study. It is possible that the formulas which performed well in comparison with our field tests would be inaccurate when compared to the results of laboratory experiments, since field tests are affected by scale effects and local heterogeneity and anisotropy. There is a need for more detailed investigations of the performance of empirical equations, including pumping and permeameter tests, CPT or DP tests near boreholes or geophysical tests to obtain information on in-situ porosity and laboratory tests on samples with different porosity.

Acknowledgements

This work has been supported by grant 2015/17/B/ST10/03233 ‘Groundwater recharge on outwash plain’ funded by National Science Centre (NCN), Poland.

References

[1] J. Sobieraj, M. Bryx, and D. Metelski, “Management of rainwater as a barrier for the development of the City of Warsaw”, *Archives of Civil Engineering*, vol. 68, no. 4, pp. 419–443, 2022, doi: 10.24425/ace.2022.143047.

[2] Z. Skrzypczak, A. Różański, I. Bagińska, and R. Pratkowiecki, “Construction of dams using the hydraulic fill method, discussion of the methodology of the Tailings Storage Facility Żelazny Most”, *Archives of Civil Engineering*, vol. 68, no. 2, pp. 227–242, 2022, doi: 10.24425/ace.2022.140639.

[3] M. Vuković and A. Soro, *Determination of hydraulic conductivity of porous media from grain size composition*. Littleton: Water Resources Publications, 1992.

[4] M. Kasenow, *Determination of Hydraulic Conductivity from Grain Size Analysis*. Littleton: Water Resources Publications, 2002.

[5] A. Szymkiewicz and A. Kryczałło, “Obliczanie współczynnika filtracji piasków i żwirów na podstawie krzywej uziarnienia: przegląd wzorów empirycznych”, *Inżynieria Morska i Geotechnika*, no. 2, pp. 110–121, 2011.

[6] R.P. Chapuis, “Predicting the saturated hydraulic conductivity of soils: a review”, *Bulletin of Engineering Geology and the Environment*, vol. 71, no. 3, pp. 401–434, 2012, doi: 10.1007/s10064-012-0418-7.

[7] K. Urumović and Sr.K. Urumović, "The referential grain size and effective porosity in the Kozeny–Carman model", *Hydrology and Earth System Sciences*, vol. 20, no. 5, pp. 1669–1680, 2016, doi: 10.5194/hess-20-1669-2016.

[8] M. Kimura, "Prediction of tortuosity, permeability, and pore radius of water-saturated unconsolidated glass beads and sands", *The Journal of the Acoustical Society of America*, vol. 143, no. 5, pp. 3154–3168, 2018, doi: 10.1121/1.5039520.

[9] X.W. Ren and J.C. Santamarina, "The hydraulic conductivity of sediments: A pore size perspective", *Engineering Geology*, vol. 233, pp. 48–54, 2018, doi: 10.1016/j.enggeo.2017.11.022.

[10] M. Arshad, M.S. Nazir, and B.C. O'Kelly, "Evolution of hydraulic conductivity models for sandy soils", *Proceedings of the Institution of Civil Engineers-Geotechnical Engineering*, vol. 173, no. 2, pp. 97–114, 2020, doi: 10.1680/jgeen.18.00062.

[11] K. Urumović, S. Borović, and D. Navratil, "Validity range and reliability of the United States Bureau of Reclamation (USBR) method in hydrogeological investigations", *Hydrogeology Journal*, vol. 28, no. 2, pp. 625–636, 2020, doi: 10.1007/s10040-019-02080-2.

[12] J.Díaz-Curiel, M.J. Miguel, B. Biosca, and L. Arévalo-Lomas, "New granulometric expressions for estimating permeability of granular drainages", *Bulletin of Engineering Geology and the Environment*, vol. 81, no. 10, pp. 1–15, 2022, doi: 10.1007/s10064-022-02897-4.

[13] K. Parylak, Z. Zieba, A. Buldys, and K. Witek, "Weryfikacja wyznaczania współczynnika filtracji gruntów niespoistych za pomocą wzorów empirycznych w ujęciu ich mikrostruktury", *Acta Scientiarum Polonorum. Architectura*, vol. 12, no. 2, pp. 43–51, 2013.

[14] F. Pliakas and C. Petalas, "Determination of hydraulic conductivity of unconsolidated river alluvium from permeameter tests, empirical formulas and statistical parameters effect analysis", *Water Resources Management*, vol. 25, no. 11, pp. 2877–2899, 2011, doi: 10.1007/s11269-011-9844-8.

[15] K. Dołżyk and I. Chmielewska, "Predicting the coefficient of permeability of non-plastic soils", *Soil Mechanics and Foundation Engineering*, vol. 51, no. 5, pp. 213–218, 2014, doi: 10.1007/s11204-014-9279-3.

[16] J. Rosas, O. Lopez, T.M. Missimer, K.M. Coulibaly, A.H. Dehwah, K. Sesler, and D. Mantilla, "Determination of hydraulic conductivity from grain-size distribution for different depositional environments", *Groundwater*, vol. 52, no. 3, pp. 399–413, 2014, doi: 10.1111/gwat.12078.

[17] J. Říha, L. Petrula, M. Hala, and Z. Alhasan, "Assessment of empirical formulae for determining the hydraulic conductivity of glass beads", *Journal of Hydrology and Hydromechanics*, vol. 66, no. 3, pp. 337–347, 2018, doi: 10.2478/johh-2018-0021.

[18] I.C. Toumpanou, I.A. Pantazopoulos, I.N. Markou, and D.K. Atmatzidis, "Predicted and measured hydraulic conductivity of sand-sized crushed limestone", *Bulletin of Engineering Geology and the Environment*, vol. 80, no. 2, pp. 1875–1890, 2021, doi: 10.1007/s10064-020-02032-1 .

[19] J. Kozeny, "Uber kapillare Leitung der Wasser in Boden", *Boden Sitzungsberichte Wiener Akademie*, vol. 136, pp. 271–306, 1927.

[20] C.S. Slichter, "Theoretical investigation of the motion of ground waters", in *The 19th Annual Report US Geophys Survey*. 1899, pp. 304–319.

[21] F. Zunker, "Das Verhalten des Bodens zum Wasser", in *Handbuch der Bodenlehre*, vol. 6. Berlin: Springer, 1930, pp. 66–220.

[22] Z. Białas and A. S. Kleczkowski, "O przydatności niektórych wzorów empirycznych dla określania współczynnika filtracji", *Archiwum Hydrotechniki*, vol. 17, no. 3, 1970.

[23] C. Cheng and X. Chen, "Evaluation of methods for determination of hydraulic properties in an aquifer–aquitard system hydrologically connected to a river", *Hydrogeology Journal*, vol. 15, no. 4, pp. 669–678, 2007, doi: 10.1007/s10040-006-0135-z.

[24] J.Y. Cheong, S.Y. Hamm, H.S. Kim, E.J. Ko, K. Yang, and J.H. Lee, "Estimating hydraulic conductivity using grain-size analyses, aquifer tests, and numerical modeling in a riverside alluvial system in South Korea", *Hydrogeology Journal*, vol. 16, no. 6, pp. 1129–1143, 2008, doi: 10.1007/s10040-008-0303-4.

[25] M.K.N. Shamsuddin, W.N.A. Sulaiman, M.F. Ramli, and F.M. Kusin, "Vertical hydraulic conductivity of riverbank and hyporheic zone sediment at Muda River riverbank filtration site, Malaysia", *Applied Water Science*, vol. 9, no. 1, pp. 1–22, 2019, doi: 10.1007/s13201-018-0880-x.

[26] T. Vienken and P. Dietrich, "Field evaluation of methods for determining hydraulic conductivity from grain size data", *Journal of Hydrology*, vol. 400, no. 1-2, pp. 58–71, 2011, doi: 10.1016/j.jhydrol.2011.01.022.

[27] J. Song, X. Chen, C. Cheng, D. Wang, S. Lackey, and Z. Xu, "Feasibility of grain-size analysis methods for determination of vertical hydraulic conductivity of streambeds", *Journal of Hydrology*, vol. 375, no. 3-4, pp. 428–437, 2009, doi: 10.1016/j.jhydrol.2009.06.043.

[28] C. Lu, X. Chen, C. Cheng, G. Ou, and L. Shu, "Horizontal hydraulic conductivity of shallow streambed sediments and comparison with the grain-size analysis results", *Hydrological Processes*, vol. 26, no. 3, pp. 454–466, 2012, doi: 10.1002/hyp.8143.

[29] R.P. Chapuis, "Estimating the in situ porosity of sandy soils sampled in boreholes", *Engineering Geology*, vol. 141-142, pp. 57–64, 2012, doi: 10.1016/j.enggeo.2012.04.015.

[30] M.A. Maroof, A. Mahboubi, E. Vincens, and A. Noorzad, "Effects of particle morphology on the minimum and maximum void ratios of granular materials", *Granular Matter*, vol. 24, no. 1, pp. 1–24, 2022, doi: 10.1007/s10035-021-01189-0.

[31] A. Gumuła-Kawęcka, B. Jaworska-Szulc, A. Szymkiewicz, W. Gorczewska-Langner, M. Pruszkowska-Caceres, R. Angulo-Jaramillo, and J. Šimůnek, "Estimation of groundwater recharge in a shallow sandy aquifer using unsaturated zone modeling and water table fluctuation method", *Journal of Hydrology*, vol. 605, art. no. 127283, 2022, doi: 10.1016/j.jhydrol.2021.127283.

[32] S. Turek, *Poradnik hydrogeologa*. Warszawa: Wydawnictwa Geologiczne, 1971.

[33] G. Kovacs, *Seepage hydraulics*. Elsevier, 1981.

[34] W. Beyer and K.H. Schweiger, "Zur Bestimmung des entwässerbaren Porenanteils der Grundwasserleiter", *Wasserwirtschaft – Wassertechnik*, vol. 19, no. 2, 1969.

[35] T.L. Youd, "Factors controlling maximum and minimum densities of sands. Evaluation of Relative Denisty and Its Role in Geotechnical Projects Involving Cohesionless Soils", in *ASTM Special Technical Publications*. American Society for Testing and Materials (ASTM), 1973, pp. 98–112.

[36] D.W. Urish, "Electrical resistivity—hydraulic conductivity relationships in glacial outwash aquifers", *Water Resources Research*, vol. 17, no. 5, pp. 1401–1408, 1981, doi: 10.1029/WR017i005p01401.

[37] J. Zheng and R.D. Hryciw, "Index void ratios of sands from their intrinsic properties", *Journal of Geotechnical and Geoenvironmental Engineering*, vol. 142, no. 12, art. no. 06016019, 2016, doi: 10.1061/(ASCE)GT.1943-5606.0001575.

[38] R.P. Chapuis and M. Aubertin, "On the use of the Kozeny - Carman equation to predict the hydraulic conductivity of soils", *Canadian Geotechnical Journal*, vol. 40, no. 3, pp. 616–628, 2003, doi: 10.1139/T03-013.

[39] T.T. Nguyen and B. Indraratna, "The role of particle shape on hydraulic conductivity of granular soils captured through Kozeny–Carman approach", *Géotechnique Letters*, vol. 10, no. 3, pp. 398–403, 2020, doi: 10.1680/jgele.20.00032.

[40] A. Revil and L.M. Cathles, "Permeability of shaly sands", *Water Resources Research*, vol. 35, no. 3, pp. 651–662, 1999, doi: 10.1029/98WR02700.

[41] F.T. Mavis and E.F. Wilsey, *A study of the permeability of sand*. University of Iowa City, 1936.

[42] K. Urumović and K.Sr. Urumović, "Comment on "HydrogeoSieveXL: an Excel-based tool to estimate hydraulic conductivity from grain-size analysis": technical note published in *Hydrogeology Journal*, 2015, 23, pp. 837–844, by JF Devlin", *Hydrogeology Journal*, vol. 25, no. 2, pp. 589–591, 2017, doi: 10.1007/s10040-016-1509-5.

[43] A. Zuber, "Obliczanie współczynnika filtracji skał sypkich z krzywej uziarnienia", in *Materiały VI Konferencji Współczesne Problemy Hydrogeologii w Polanicy Zdroju*. Wrocław: Oficyna Wydawnicza Sudety, 1993, pp. 415–419.

[44] R.P. Chapuis, "Predicting the saturated hydraulic conductivity of sand and gravel using effective diameter and void ratio", *Canadian Geotechnical Journal*, vol. 41, no. 5, pp. 787–795, 2004, doi: 10.1139/t04-022.

[45] M. Mbonimpa, M. Aubertin, R.P. Chapuis, and B. Bussière, "Practical pedotransfer functions for estimating the saturated hydraulic conductivity", *Geotechnical and Geological Engineering*, vol. 20, pp. 235–259, 2002, doi: 10.1023/A:1016046214724.

[46] I.A. Palagin, "Opredelenie vodopronicaemosti zernistych materialov i niesviazlych gruntov", *Gidrotehnicheskoje Stroitielstvo*, no. 3, pp. 41–42, 1964.

[47] A.L. Gol'din and L.N. Rasskazov, *Proektirovanie gruntovych plotin*. Moskwa: Energoatomizdat, 1987.

[48] I.A. Skabałłanowicz, *Gidrogeołogiczeskije rasczety po dinamike podzemnych wod*. Moskwa, 1960.

[49] K. Terzaghi, "Principles of soil mechanics: III. Determination of permeability of clay", *Engineering News Records*, vol. 95, no. 21, pp. 832–836, 1925.

[50] A.A. Shahabi, B.M. Das, and A.J. Tarquin, "An empirical relation for coefficient of permeability of sand", in *Proceedings of the Fourth Australia-New Zealand Conference on Geomechanics*, *Perth, 14-18 May 1984*. 1984, pp. 54–57.

[51] W. Beyer, "Zur Bestimmung der Wasserdurchlässigkeit von Kiesen und Sanden aus der Kornverteilungskurve", *Wasserwirtschaft – Wassertechnik*, vol. 14, no. 6, 1964.

[52] J.P. Powers, A.B. Corwin, P.C. Schmall, and W.E. Kaeck, *Construction dewatering and groundwater control: new methods and applications*. John Wiley & Sons, 2007, doi: 10.1002/9780470168103.ch28.

[53] A. Hazen, "Some physical properties of sand and gravel, with special reference to their use in filtration", in *Massachusetts State Board of Health. 24th Annual Report*. Boston, 1892, pp. 539–556.

[54] W.C. Krumbein and G.D. Monk, "Permeability as a function of the size parameters of unconsolidated sand", *Transactions of the AIME*, vol. 151, no. 1, pp. 153–163, 1943.

[55] F.D. Masch and K.J. Denny, "Grain size distribution and its effect on the permeability of unconsolidated sands", *Water Resources Research*, vol. 2, no. 4, pp. 665–677, 1966, doi: 10.1029/WR002i004p00665.

[56] F. Seelheim, "Methoden zur Bestimmung der Durchlässigkeit des Bodens", *Zeitschrift für Analytische Chemie*, vol. 19, no. 1, pp. 387–418, 1880.

[57] J. Zieschang, "Die Bestimmung der Wasserdurchlässigkeit von Lockergesteinsgrundwasserleitern", *Zeitschrift für Angewandte Geologie*, vol. 10, no. 7, pp. 364–370, 1964.

[58] P. Bischoff, H. Fliegner, L. Richter, and H. Wehner, "Die Ermittlung des Durchlässigkeitsbeiwert "kf" mittels elektronicher Datenverarbeitungsanlagen aus den Ergebnissen von Siebanalysen", *Zeitschrift für Angewandte Geologie*, vol. 14, no. 2, pp. 88–93, 1968.

[59] W.C. Krumbein, and L.L. Sloss, *Stratigraphy and sedimentation*. San Francisco: W. H. Freeman, 1963.

[60] A.C. Muller and S. Guido, "Uczenie nienadzorowane i przetwarzanie wstępne", in *Machine learning, Python i data science*. Gliwice: Helion SA, 2021, pp. 150–167.

[61] P. Bruce, A. Bruce, and P. Gedeck, *Statystyka praktyczna w data science*, 2nd ed. Gliwice: Helion SA, 2021.

Przepuszczalność gruntów piaszczystych oszacowana na podstawie rozkładu wielkości cząstek i pomiarów terenowych

Słowa kluczowe: przepływ wód podziemnych, krzywa uziarnienia, współczynnik filtracji

Streszczenie:

Dokładne oszacowanie przepuszczalności gruntu (k) ma kluczowe znaczenie w wielu zastosowaniach geotechnicznych. Empiryczne i teoretyczne równania oparte na rozkładzie uziarnienia (PSD) umożliwiają szybką i tanią wstępną ocenę przepuszczalności gruntów ziarnistych, jednak wyniki otrzymane z różnych wzorów dostępnych w literaturze często wykazują znaczne rozbieżności. Chociaż opublikowano kilka badań porównawczych na ten temat, nie można wyciągnąć jednoznacznych wniosków dotyczących zgodności równań predykcyjnych z pomiarami przepuszczalności wykonanymi bezpośrednio w terenie. Wiele wzorów wymaga uwzględnienia współczynnika porowatości jako parametru wejściowego, co jest trudne do uzyskania w przypadku gruntu ziarnistego in-situ. W niniejszej pracy zastosowano 30 równań predykcyjnych do oszacowania przepuszczalności gleby

piaszczystej na terenie równiny sandrowej, zlokalizowanej w pobliżu miejscowości Cekcyn w Borach Tucholskich, w północnej Polsce. Badania realizowane były w ramach projektu badawczego dotyczącego określenia zasilania wód podziemnych. Równania predykcyjne podzielono na 5 grup ze względu na ich strukturę oraz wymagane parametry wejściowe. Wzory empiryczne wykorzystano do oszacowania oczekiwanego zakresu porowatości in-situ. Otrzymane wartości przepuszczalności porównano z wynikami pomiarów in-situ wykonanych za pomocą permeametru Aardvark oraz uzyskanych w wyniku próbnego pompowania. Stwierdzono istotne różnice w wynikach uzyskanych poszczególnymi wzorami oraz ich wrażliwość na współczynnik porowatości. Najlepszą zgodność wyników empirycznych z pomiarami in-situ uzyskano dla tych grup formuł, które nie uwzględniają porowatości lub uwzględniają jedynie stopień zagęszczenia, gdyż metody te opracowano pierwotnie na podstawie wyników badań terenowych. Jak wykazano w pracy, większość metod opartych na pomiarach laboratoryjnych przewiduje k niższe niż pomiary in-situ, czego powodem między innymi może być anizotropia i niejednorodność gruntu, który zwiększa przepuszczalność poziomą in situ, ze względu na obecność poziomych warstw lub soczewek o małej skali. Cechy te są trudne do uchwycenia za pomocą wzorów opartych na krzywych PSD.

Received: 2023-04-03, Revised: 2023-05-17